



# CHALMERS

## Chalmers Publication Library

### **Study of the Characteristic Impedance of Gap Waveguide Microstrip Line**

This document has been downloaded from Chalmers Publication Library (CPL). It is the author's version of a work that was accepted for publication in:

**7th European Conference on Antennas and Propagation, EuCAP 2013, Gothenburg, Sweden, 8-12 April 2013**

Citation for the published paper:

Raza, H. ; Yang, J. ; Kildal, P. (2013) "Study of the Characteristic Impedance of Gap Waveguide Microstrip Line". 7th European Conference on Antennas and Propagation, EuCAP 2013, Gothenburg, Sweden, 8-12 April 2013

Downloaded from: <http://publications.lib.chalmers.se/publication/177761>

Notice: Changes introduced as a result of publishing processes such as copy-editing and formatting may not be reflected in this document. For a definitive version of this work, please refer to the published source. Please note that access to the published version might require a subscription.

Chalmers Publication Library (CPL) offers the possibility of retrieving research publications produced at Chalmers University of Technology. It covers all types of publications: articles, dissertations, licentiate theses, masters theses, conference papers, reports etc. Since 2006 it is the official tool for Chalmers official publication statistics. To ensure that Chalmers research results are disseminated as widely as possible, an Open Access Policy has been adopted. The CPL service is administrated and maintained by Chalmers Library.

(article starts on next page)

# Study of the Characteristic Impedance of Gap Waveguide Microstrip Line Realized With Square Metal Pins

Hasan Raza<sup>1</sup>, Jian Yang<sup>1</sup>, Per-Simon Kildal<sup>1</sup>

<sup>1</sup>Department of Signals and Systems, Chalmers University of Technology, Gothenburg, Sweden.

**Abstract**— This paper addresses how to define the numerical ports in the gap waveguide microstrip line, and also a study of its characteristic impedance when the parallel-plate stopband is realized by using metal pins. The results presented here are produced using commercially available EM simulators. The paper also includes a study of how to minimize the effect of the transverse locations of the pin structure under the microstrip line, relative to the location of the strip.

**Index Terms**—gap waveguide; microstrip line; packaging

## I. INTRODUCTION

Recently, the gap waveguide technology has been introduced for making low loss circuits at millimeter and sub-millimeter waves [1]-[3]. This kind of transmission line not only provides low loss propagation along the line, but also makes the circuits completely enclosed in a package containing large cavities but without having any cavity modes. This fact can be used to package microstrip circuits [4][5], and even to improve the Q of microstrip line filters [6]. The gap waveguide has special advantages in realizing practically useful packaged inverted microstrip lines. Such inverted gap waveguide microstrip line (also being referred to as an inverted microstrip gap waveguide) is realized by having a dielectric layer over a periodic pattern of pins [3], and there is an air gap between the top metal plate and the substrate material supporting the microstrip line. The pin structure works as an artificial magnetic surface (AMC), so the microstrip gap waveguide is an AMC-packaged inverted (or suspended) microstrip line. The AMC-type pins surface produce together with the upper metal surface a stopband for all types of parallel-plate modes, except for the quasi-TEM mode along the microstrip line. The pin AMC can also be realized in other ways than by using pins, such as mushrooms [7], bed of springs [8] and zigzag wires [9]. It is also possible to integrate mushrooms in the same surface as the microstrip line [10]. The numerical design of microstrip gap waveguides are complicated because there are no ports in common EM solvers that are suited for the specific quasi-periodic geometry

This paper addresses how to define the numerical ports in the gap waveguide microstrip line, and also a study of its characteristic impedance. The results presented are produced using CST Microwave Studio. Through CST, the line impedance can be calculated at the ports. Similarly, another

commercially available simulator, HFSS, also give the port impedance as a function of frequency. A preliminary numerical study of the characteristic impedance of the groove and ridge gap waveguide has been done in [11], by comparing results with similar hollow waveguides, i.e. the standard rectangular waveguide and the normal ridge waveguide with solid metal walls. Similarly, the characteristic impedance of the gap waveguide microstrip line can be estimated through the inverted microstrip line model as mentioned in [12]. The purpose of this work is also to investigate methods to minimize the effect of the lateral location of the pins relative to the microstrip line.

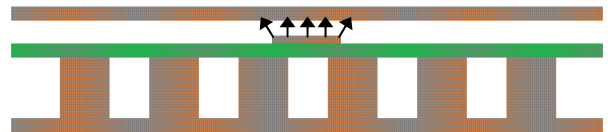


**Figure 1: Basic configuration of gap waveguide microstrip line. Grey color represents metal, and green color the substrate. The arrows indicate the field lines of the quasi-TEM mode.**

## II. GEOMETRY AND MODELING

The geometry of the gap waveguide microstrip line is shown in Fig. 1. The periodic pattern of pins under the substrate material creates a PMC layer that forces the waves to propagate only in the narrow gap between the top metal plate and the metal above the substrate material, in the form of a quasi-TEM mode. The dispersion diagram determines the major characteristics of the gap waveguide technology. By using Eigen mode solver in CST microwave studio, the dispersion diagram is calculated as a function of frequency for specific choices of dimensions of the gap waveguide. We will show results both when the microstrip line is aligned to be parallel with the pin rows, and also when it makes an angle of  $45^\circ$  with the row, and we will study the differences in particular with respect to the lateral location of the microstrip line relative to the pins. We will first present and discuss the parallel to pin rows case, but the results for the  $45^\circ$  case is shown in the same figures side-by-side, in order to better see the differences.

The geometry of the parallel example is shown in Fig. 3 a. The pin height is 5 mm and width is 3 mm. The distance between two pins is 3.5 mm. The substrate material is 0.762 mm thick TMM3 having  $\epsilon_r$  equal to 3.27. The air gap is 0.5 mm. We see that the stopband of the parallel-plate modes for this specific case is between 9 and 18 GHz, with only one fundamental mode propagating within the stopband..

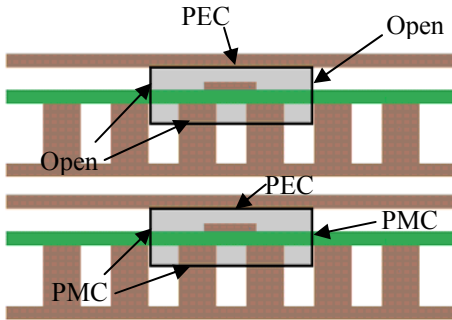


**Figure 2: Port definitions used in CST (upper) and in HFSS (lower)**

### III. PORT CONFIGURATION AND S-PARAMETERS

The waveguide ports available in both CST and in HFSS have been attached to the gap waveguide using the same principle as defined for normal microstrip line in [13][14]. In CST, the port is defined at the edge of the microstrip line, with open boundary condition at that side. In HFSS, the port dimensions are same but finite length PMC boundary conditions applied on three sides of the port, as shown in Fig. 2. The simulations were done on inverted microstrip gap waveguides with a length of 76.25 mm and the width of the line is 2.2 mm, see Fig. 4a.

However, the location of the interface for the waveguide port and its size should be treated with care. A parametric study on  $k_1$ ,  $k_2$  and  $g_1$  which defines the size and location of the port (see Fig. 5a) has been carried out. The best result appears when  $k_1 = 2p$ ,  $k_2 = d/2$  and  $g_1 = p/4$ , where  $p$  is the spacing between the walls of the pins and  $d$  is the height of the pins, as shown in Fig. 6a. Fig. 7a shows the S-parameters for the four cases: microstrip line above the pins, at the edge of pins, in between two pins and inverted microstrip line with ideal PMC boundary underneath. We can see that the reflection coefficients  $S_{11}$  of the straight gap waveguide microstrip line is different for each case, meaning that the characteristic impedance of the line depends on the pin location relative to the microstrip line. The transmission coefficient  $S_{21}$  is very low in each case, i.e. around -0.2 dB at lower frequencies and goes down to -0.75 dB at the higher frequencies within the stopband.

For the calculations of the characteristic impedance, the same method as mentioned in [11] has been applied, although the magnitude of reflection coefficient should be smaller than 0.2 for best accuracy [15]. By using this approach, the characteristic impedance of the gap waveguide microstrip line becomes as shown in Fig. 8a. We have included three reference impedances: a) the impedance provided by CST when the ports are on PMC boundary condition, b) the port impedance as shown in Fig. 4a and Fig. 5a, and c) the impedance of the inverted microstrip line estimated through the model describe

in [12]. We see that there is a significant effect of the pins and their location relative to the microstrip line, especially at higher frequencies in the stopband. One way to investigate the pin effect without changing the port location is to make the structure as shown in Fig. 9a. The locations of the ports are fixed now, only the bended portion of the gap waveguide microstrip line changes over the pin. Fig. 10a shows the reflection coefficient for each case when the location of the bended portion of the gap waveguide microstrip line changes over the pins. The result clearly shows that the peaks of the reflection coefficients typically varies with the lateral location relative to the pins between -15 dB and -20 dB over the best parts of the band.

### IV. GAP WAVEGUIDE MICROSTRIP LINE FOLLOWS 45° TO THE PIN STRUCTURE

Several methods have been analyzed to minimize the pin effect on the gap waveguide microstrip line. Among them is to make the microstrip line follows 45° degree to the pin pattern as shown in Fig. 4b. After following similar procedures as in previous sections, we have found the best port size and location as shown in Fig 6b and the reflection coefficient is much lower than for the previous parallel case. The reflection coefficients for each strip location relative to pins are shown in Fig. 7b. Note that the pin geometry is not the same as for the parallel case. Substrate material is the same, i.e. 0.381 mm thick TMM3. However, pin width and the distance between two pins have been reduced to 1.714 mm. The height of the pins is 5 mm whereas the air gap between the strip and the metal top lid is 0.25 mm. Using the same method, as in the previous section, the characteristic impedance has been calculated by the reflection coefficients and the corresponding port impedances for each case and is shown in Fig. 8b. It can be seen that variation in the impedances for the case when the line is following 45° to the periodic pins is smaller than before. Similarly, the microstrip line with two 90° bends has also been analyzed when located 45° with respect to the pins, as shown in Fig. 9b. The reflection coefficient is shown in Fig. 10b. Generally we see that the 45° orientation is better with respect to both variation of characteristic impedance and input reflection coefficient. Note the reflection coefficients for the PMC reference case in all graphs. This is much lower than for the practical pin realizations.

### V. CONCLUSION

Numerical studies have been done to determine the characteristic impedance of gap waveguide microstrip line over PMC and different pin configurations. So far the results show that the reflection coefficient is strongly affected by the position of the microstrip line with respect to the row of pins. The affect is for a two-port case in the order of -15 dB, so that for each port this corresponds to -21 dB. This variation is large, and we have been able to reduce it slightly by location the microstrip line diagonally 45° relative to the pin rows. However, we had to change the dimensions somewhat not to change the stopband too much. The paper presents only preliminary results, and it is clear that the pin period and relative location between pins and microstrip line has an undesired effect on the performance of the line, i.e. the effect is

in most cases too large. Therefore, it is important to work further to try to minimize these affects in order to arrive to a more generic inverted gap waveguide microstrip line.

ACKNOWLEDGMENT

This work has been supported by The Swedish Research Council VR and Pakistan’s NESCOM scholarship program.

REFERENCES

[1] P.-S. Kildal, A. Uz Zaman, Eva Rajo, E. Alfonso, A. Valero Nogueira, "Design and Experimental Verification of Ridge Gap Waveguide in Bed of Nails for Parallel Plate Mode Suppression", IET Microwave Antennas and Propag., Vol. 5, No. 3, pp. 262-270, March 2011.

[2] P.-S. Kildal, E. Alfonso, A. Valero, and E. Rajo, "Local Metamaterial-Based Waveguides in Gaps Between Parallel Metal Plates", IEEE Antennas and Wireless Propagation Letters, 2009, (8), pp. 84 - 87.

[3] P.-S. Kildal, "Three metamaterial-based gap waveguides between parallel metal plates for mm/submm waves", 3rd European Conference on Antennas and Propagation, 2009. EuCAP 2009. Berlin, Germany, 23-27 March 2009.

[4] E. Rajo, A. Uz Zaman, P.-S. Kildal, "Parallel plate cavity mode suppression in microstrip circuit packages using a lid of nails", IEEE Microwave & Wireless Comp. Lett., Vol. 20, No. 1, pp. 31-33, Dec. 09.

[5] A. U. Zaman, J. Yang, and P.-S. Kildal, "Using Lid of Pins for Packaging of Microstrip Board for Descrambling the Ports of Eleven Antenna for Radio Telescope Applications", 2010 IEEE international Symp. on Antennas Propag., Toronto, Canada, July 11-17, 2010.

[6] A. Algaba Brazález, A. Uz Zaman, P.-S. Kildal, "Improved Microstrip Filters Using PMC Packaging by Lid of Nails", IEEE Transactions on

Components, Packaging and Manufacturing Technology, Vol. 2, No. 7, July 2012.

[7] E. Rajo-Iglesias, P.-S. Kildal, "Numerical studies of bandwidth of parallel plate cut-off realized by bed of nails, corrugations and mushroom-type EBG for use in gap waveguides", IET Microwaves, Antennas & Propagation, Vol. 5, No 3, pp. 282-289, March 2011.

[8] E. Rajo-Iglesias, P.-S. Kildal, A.U. Zaman and A. Kishk, "Bed of springs for packaging of microstrip circuits in the microwave frequency range", IEEE Transactions on Components, Packaging and Manufacturing Technology, Vol. 2, No. 10, October 2012.

[9] E. Rajo-Iglesias, E. Pucci, A. Kishk, and P.-S. Kildal, "Suppression of parallel plate modes for low frequency microstrip circuit packaging using lid of printed zigzag wires", submitted to IEEE Microwave and Wireless Components Letters, Dec 2012.

[10] E. Pucci, E. Rajo-Iglesias, P.-S. Kildal, "New Microstrip Gap Waveguide on Mushroom-Type EBG for Packaging of Microwave Components", IEEE Microwave and Wireless Components Letters, Vol. 22, No. 3, pp. 129-131, March 2012.

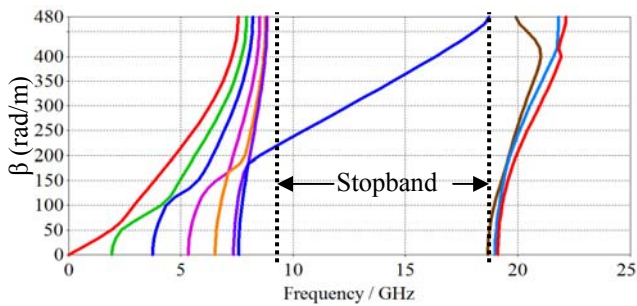
[11] H. Raza, J. Yang, P.-S. Kildal, E. Alfonso, "Resemblance Between Gap Waveguides and Hollow Waveguides", Submitted to IET Microwave, Antennas & Propagation, September 2012.

[12] R. S. Tomar, and P. Bhartia, "New Quasi-Static Models for the Computer Aided Design of Suspended and Inverted Microstrip Lines", IEEE Trans. on Microwave Theory and Tech., Vol. MTT - 35, No. 4, April 1987, pp. 453 - 457, and corrections No. 11, Nov. 1987, p. 1076.

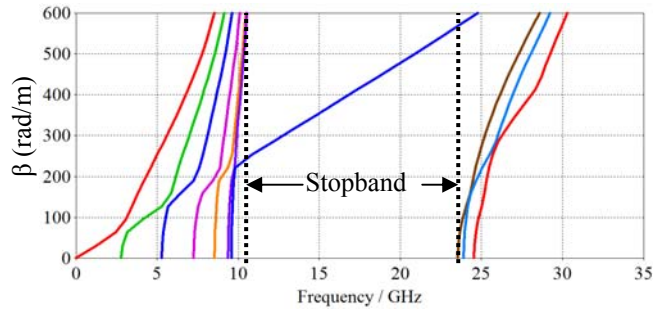
[13] CST Microwave Studio, Computer Simulation Technology, Framingham, MA, 2011 [Online]. Available: <http://www.cst.com>.

[14] Ansoft HFSS: version 12, [Online]. Available: <http://www.ansys.com/>.

[15] P.-S. Kildal, "Foundations of Antennas – A Unified Approach", 2nd Edition, Section 2.7, pg. 86, Studentlitteratur, 2000.

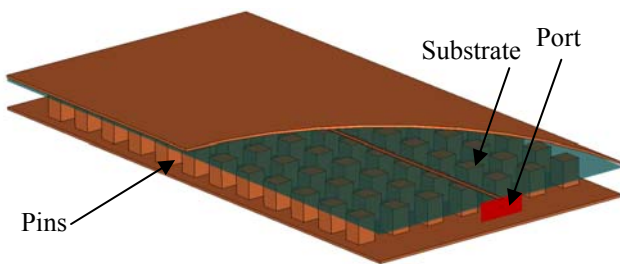


(a)

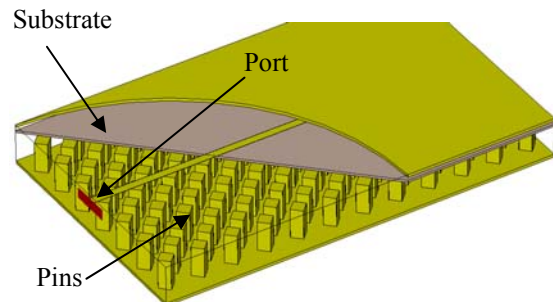


(b)

Figure 3: Dispersion diagram of gap waveguide microstrip line.



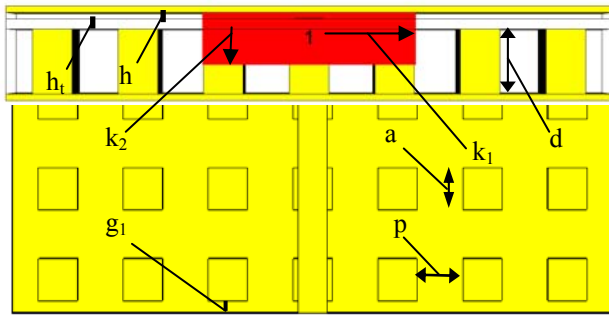
a) Strip parallel with lines of grid



b) Strip making 45° with lines of grid.

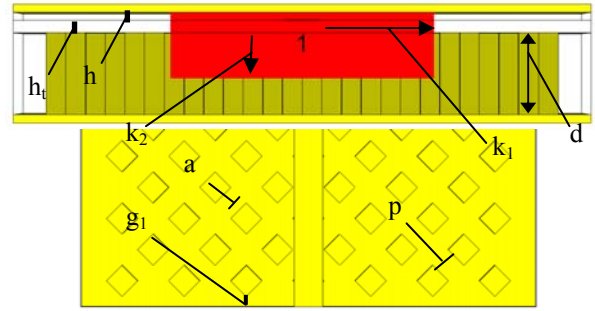
Figure 4: Port configuration for simulating the S – parameters of the gap waveguide microstrip line.





a	3 mm
p	3.5 mm
d	5 mm
h	0.5 mm
h <sub>t</sub>	0.762 mm
ε <sub>r</sub>	3.27

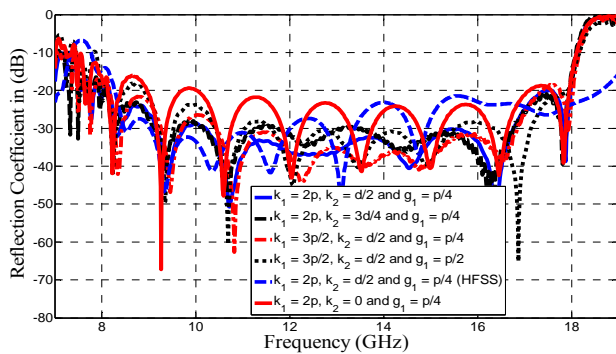
a) Strip parallel with lines of grid



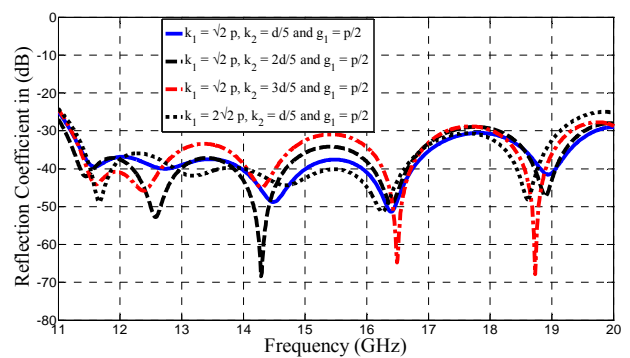
a	1.714 mm
p	1.714 mm
d	5 mm
h	0.25 mm
h <sub>t</sub>	0.381 mm
ε <sub>r</sub>	3.27

b) Strip making 45° with lines of grid.

**Figure 5: Definition of port geometry relative to the pins and microstrip line, cross-sectional view (upper case) and top view (lower case)**

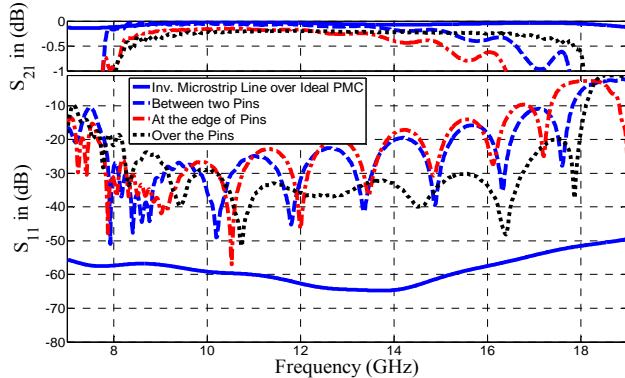


a) Strip parallel with lines of grid

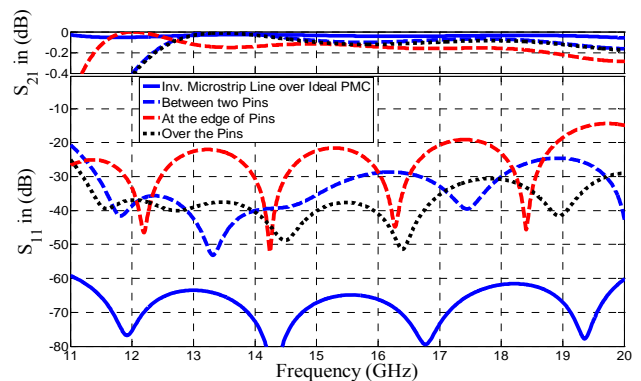


b) Strip making 45° with lines of grid.

**Figure 6: Reflection coefficient for different port geometries for a location with the microstrip line directly over a pin row.**

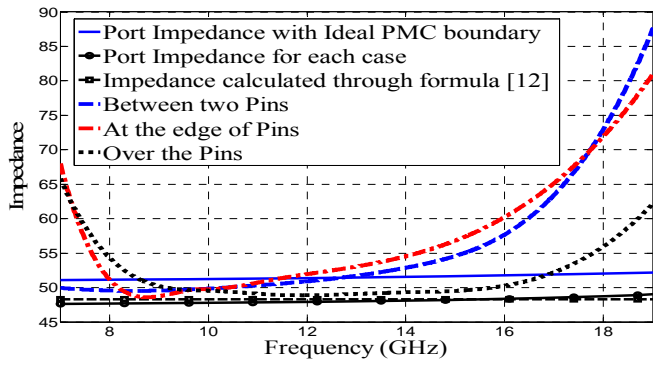


a) Strip parallel with lines of grid

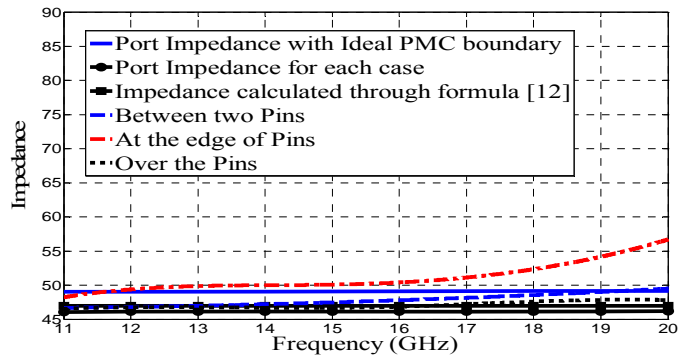


b) Strip making 45° with lines of grid.

**Figure 7: S-parameters of the waveguide in Figure 4 for different locations of the microstrip line relative to the pin rows.**

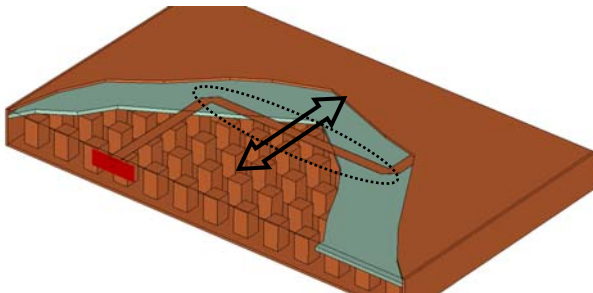


a) Strip parallel with lines of grid

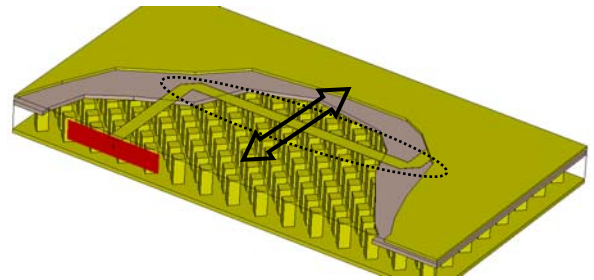


b) Strip making 45° with lines of grid.

**Figure 8: Characteristic impedance of the gap waveguide microstrip line in Figure 4 for different locations of the strip relative to the pins (curved lines), and for three reference cases (straight lines).**

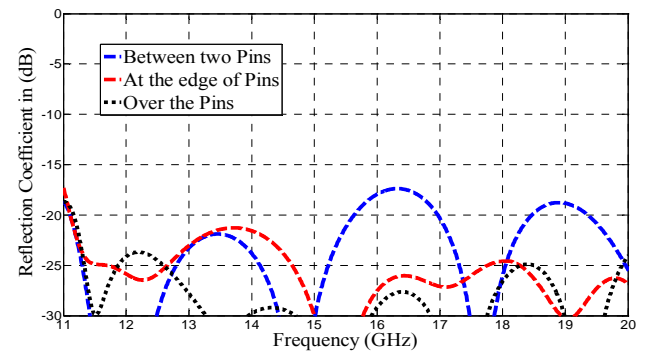
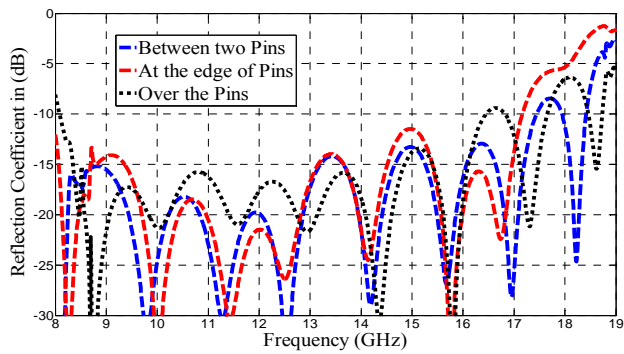
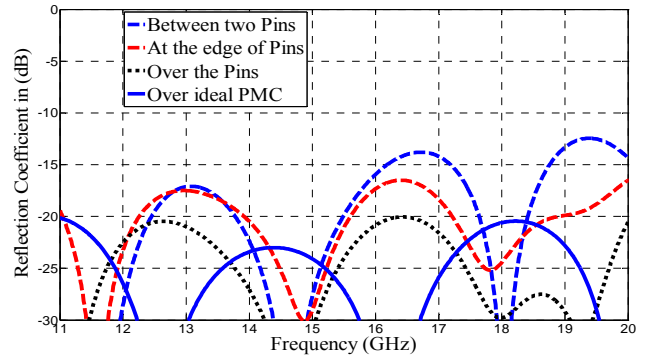
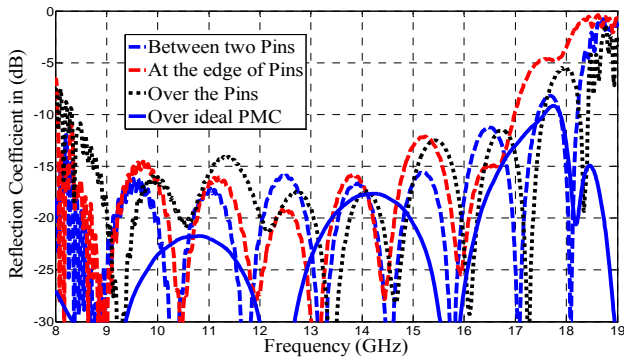


a) Strip parallel with lines of grid



b) Strip making 45° with lines of grid.

**Figure 9: Two 90° degree bend structure of gap waveguide microstrip line.**



a) Strip parallel with lines of grid

b) Strip making 45° with lines of grid.

**Figure 10: Reflection coefficient of the two 90° degree bend structure of gap waveguide microstrip line, with CST (upper) and with HFSS (lower).**